

Exploring different regimes in finite-size scaling of the droplet condensation-evaporation transition

Johannes Zierenberg* and Wolfhard Janke†

Institut für Theoretische Physik, Universität Leipzig, Postfach 100 920, D-04009 Leipzig, Germany

(Received 23 April 2015; published 27 July 2015)

We present a finite-size scaling analysis of the droplet condensation-evaporation transition of a lattice gas (in two and three dimensions) and a Lennard-Jones gas (in three dimensions) at fixed density. Parallel multicanonical simulations allow sampling of the required system sizes with precise equilibrium estimates. In the limit of large systems, we verify the theoretical leading-order scaling prediction for both the transition temperature and the finite-size rounding. In addition, we present an emerging intermediate scaling regime, consistent in all considered cases and with similar recent observations for polymer aggregation. While the intermediate regime locally may show a different effective scaling, we show that it is a gradual crossover to the large-system scaling behavior by including empirical higher-order corrections. This implies that care has to be taken when considering scaling ranges, possibly leading to completely wrong predictions for the thermodynamic limit. In this study, we consider a crossing of the phase boundary orthogonal to the usual fixed temperature studies. We show that this is an equivalent approach and, under certain conditions, may show smaller finite-size corrections.

DOI: [10.1103/PhysRevE.92.012134](https://doi.org/10.1103/PhysRevE.92.012134)

PACS number(s): 05.70.Fh, 02.70.Uu, 64.60.an, 64.60.qe

I. INTRODUCTION

The limit of large systems, or the thermodynamic limit, is of general interest when studying finite systems. It is this limit that is commonly accessible to experiments. Recent developments in experimental and simulation techniques open the door to mesoscopic length scales [1]. Here, general concepts of finite-size scaling may be tested and verified. Considering, for example, the equilibrium properties of several homopolymers, the aggregation transition temperature was shown to exhibit systematic finite-size effects that deviate from the expected behavior for particle gas systems [2]. It was argued that the observed scaling is valid for intermediate system sizes, where the aggregate includes most of the polymers, but in the limit of increasing polymer number the particle picture should be recovered. On the other hand, it is a reasonable assumption that the intermediate regime should be also apparent for particle gas condensation, which will be a main focus of the present paper.

First-order phase transitions in spin systems are usually separating homogeneous phases, which leads in general to finite-size scaling corrections on the order of the inverse system volume. Exceptions occur, for example, if the low-temperature phase is exponentially degenerated [3]. The general situation changes when we consider a phase transition between a homogeneous phase and a mixed phase, as in the case of the droplet condensation-evaporation transition separating a supersaturated gas phase and a mixed phase consisting of a single droplet in equilibrium with surrounding vapor. There exists a large amount of theoretical literature on this topic about the leading-order scaling behavior of large systems [4–6] with origins already in the 1980s [7]. Usually, a system at fixed temperature is considered, estimating the transition density at which a single macroscopic droplet forms. In the limit of very large systems, this transition density is supposed to have finite-size corrections of the order $V^{-1/(d+1)}$, while the rounding of the transition should scale with $V^{-d/(d+1)}$. The former was numerically verified to leading order at fixed

temperature for a lattice gas [5,8–10]. Several studies of a three-dimensional Lennard-Jones gas [11–13] also verified the finite-size corrections of the transition density. For a fixed density, the scaling of the transition temperature was demonstrated for the two- and three-dimensional lattice gas [14], while the scaling exponent of the finite-size rounding could not be verified. There exist complementary microcanonical studies of the Ising model at fixed density (or magnetization) [15,16], demonstrating that the occurring transition shows signatures of a first-order transition.

The present study aims to fill the gap with respect to the finite-size scaling of the droplet condensation-evaporation transition at fixed density and the gradual crossover from an effective intermediate regime to the asymptotic large-system limit. In order to draw general conclusions, we consider a lattice-gas model in two and three dimensions as well as a Lennard-Jones gas in three dimensions. We will show that the proposed scaling behavior of the transition temperature and rounding is numerically recaptured in the limit of large (but achievable) system sizes for all dimensions and models considered. Where possible, we will directly compare to analytic solutions or low-temperature series expansions. In addition, we discuss an emerging intermediate scaling regime, best visible in the rounding of the transition and consistent with recent observations of finite-size effects in polymer aggregation [2]. This regime with effective local scaling behavior and the gradual crossover to the large-system regime may be described by the finite-size scaling behavior when including empirical higher-order correction terms.

The remaining part of this paper is organized as follows. In Sec. II we briefly recapture the main leading-order results from the literature at fixed temperature and convert them to the scenario of fixed density. After describing our models and methods in Sec. III, we will present our results in Sec. IV and finish with the conclusions in Sec. V.

II. THEORY

We consider a d -dimensional liquid-vapor system of N particles in a (periodic) box of volume V , where for sufficiently dilute systems the condensation-evaporation transition

*johannes.zierenberg@itp.uni-leipzig.de

†wolfhard.janke@itp.uni-leipzig.de

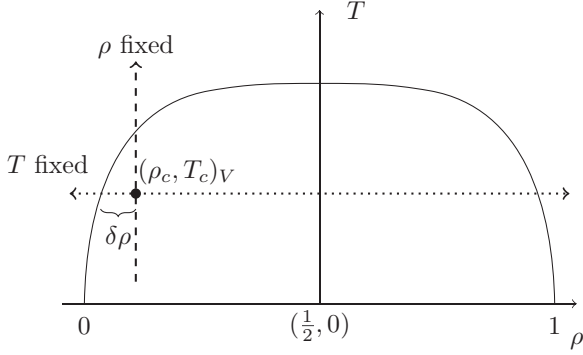


FIG. 1. Sketch of the infinite system-size transition (solid line) together with the finite-size scaling directions in either the density (T fixed) or temperature (ρ fixed). The transition line may be understood as $T_0(\rho)$ or similarly $\rho_0(T)$. At the crossing point of both schemes a finite system of size V may be constructed for which $(\rho, T) = (\rho_c, T_c)_V$ corresponds to the finite-size condensation-evaporation transition.

separates a homogeneous supersaturated gas phase from a mixed phase of a droplet in equilibrium with surrounding bulk gas. At fixed density, this occurs at the condensation-evaporation transition temperature T_c . However, the usual description of this problem is in the language of a grand-canonical scheme, considering a fixed temperature and variable density (or in case of a lattice gas equivalently the magnetization of the Ising model) with the finite-size transition density ρ_c . This is orthogonal to the scenario of a fixed density with variable temperature. Figure 1 shows a sketch of the infinite-size phase boundary $T_0(\rho)$ or $\rho_0(T)$ and the different scenarios crossing it for finite system sizes. It needs to be mentioned that both schemes are working in the canonical ensemble for each point (ρ, T) . So in fact, any finite-size transition point $(\rho_c, T_c)_V$ belongs to one fixed- T and one fixed- ρ scheme, simultaneously. The same holds for any canonical function $f(\rho, T)$. Thus, the orthogonal crossing schemes are equivalent and we may translate a functional dependence $f(\rho, T)V^\alpha = 1$ from one scheme to another by a Taylor series expansion. Then, expanding around some T^* yields

$$V^{-\alpha} = f(\rho, T^*) + f'(\rho, T^*)(T - T^*) + \dots, \quad (1)$$

which may be solved for T . The remaining task is to identify and evaluate suitable functional dependencies.

Using this procedure, we will recapture for a fixed density $\rho = N/V$ the finite-size correction to the transition temperature $T_c - T_0 \propto N^{-1/(d+1)}$ and the scaling of the finite-size rounding (or width of the finite-system transition region) $\Delta T = T - T_c \propto N^{-d/(d+1)}$. This is directly related to the linear extension of the droplet $R \propto N^{1/(d+1)}$, which becomes the relevant length scale for large system sizes.

A. Finite-size scaling of the droplet condensation-evaporation transition

Biskup *et al.* [4] showed for a d -dimensional liquid-vapor system in equilibrium a vanishing probability of intermediate-sized droplets. This was proven rigorously for the lattice-gas

interpretation of the two-dimensional (2D) Ising model and justifies the restriction of the discussion to two relevant phases: the homogeneous gas phase and the mixed phase of a single macroscopic droplet in equilibrium with a bulk gas surrounding it. At coexistence both phases are equally probable and in general (finite volume) the dominance of either phase is the solution of a saddle-point problem (see also Ref. [6]). Choosing a *fixed temperature* T , we consider a system at supersaturated density $\rho = N/V$ with particle excess $\delta N = N - N_0 = \delta \rho V$, where $\rho_0 = N_0/V$ is the equilibrium density of the infinite-system gas phase at this temperature. In fact, the particle excess is temperature dependent, see Fig. 1. A fraction $\lambda \in [0, 1]$ of this particle excess is considered to be in the single macroscopic droplet, i.e., $\delta N_D = \lambda \delta N$, while the remaining excess is in the gas phase such that $\delta N = \delta N_D + \delta N_G$. Up to higher-order corrections from surface and density fluctuations as well as translational entropy of the droplet motion, Biskup *et al.* [4] introduced a rescaled (size-independent) density

$$\Delta = \frac{(\rho_L - \rho_0)^{\frac{d-1}{d}} (\delta N)^{\frac{d+1}{d}}}{2\hat{\kappa}\tau_W V}, \quad (2)$$

with the infinite-system liquid and gas densities ρ_L and ρ_0 , the Wulff-shape surface free-energy per unit volume τ_W and the (reduced) isothermal compressibility $\hat{\kappa}$, see also Ref. [10]. Here, only δN is variable and the remaining parameters are constants encoding all system-specific details, such as the droplet shape. In the limit of large system sizes, they calculate the fraction of particles in the largest droplet $\lambda(\Delta)$ as a universal function of Δ . At the transition density $\Delta_c = \frac{1}{d} \left(\frac{d+1}{2}\right)^{(d+1)/d}$ the system changes between the vapor phase ($\lambda = 0$) and the mixed phase [$\lambda_c = 2/(d+1)$].

Now consider a *fixed density* ρ with varying temperature T . Then the system-specific constants become functions of the temperature, namely $\rho_i(T)$, $\hat{\kappa}(T)$, $\tau_W(T)$, and $\delta N(T) = [\rho - \rho_0(T)]V$. The temperature-dependent particle excess may be understood by the fact that for decreasing temperature (fixed density) the difference $\delta \rho$ increases and with it the supersaturation, see also Fig. 1. We may rewrite Eq. (2) as

$$\Delta^{\frac{d}{d+1}} V^{-\frac{1}{d+1}} = f(\rho, T), \quad (3)$$

where we identify

$$f(\rho, T) = \frac{\rho - \rho_0(T)}{\rho_L(T) - \rho_0(T)} \left(\frac{[\rho_L(T) - \rho_0(T)]^2}{2\hat{\kappa}(T)\tau_W(T)} \right)^{\frac{d}{d+1}}. \quad (4)$$

At the condensation-evaporation transition, $\Delta = \Delta_c$ is constant and the left-hand side of Eq. (3) is depending only on the system size V . Then, for a fixed finite system size, a suitable combination of T and ρ solves Eq. (3) yielding the finite-size transition point at $(\rho, T) = (\rho_c, T_c)_V$ in Fig. 1. This transition point may be obtained either numerically exact or by a Taylor expansion. Keeping $\rho = N/V$ constant, we proceed by expanding $f(\rho, T)$ in Eq. (3) around the infinite-system transition temperature T_0 , where $\rho_0(T_0) = \rho$ and thus $f(\rho, T_0) = 0$. Solving for the finite-size transition temperature $T = T_c$ yields

$$T_c = T_0 + \frac{\Delta_c^{\frac{d}{d+1}}}{f'(\rho, T_0)} V^{-\frac{1}{d+1}} + \mathcal{O}(V^{-\frac{2}{d+1}}). \quad (5)$$

In terms of the number of particles this means to first order

$$T_c - T_0 \propto N^{-\frac{1}{d+1}}. \quad (6)$$

We need to emphasize that Eq. (3) is only the leading-order result. Numeric tests at fixed temperature already showed apparent higher-order corrections [8–10].

For the Ising model, we can go a little further and evaluate the leading finite-size scaling explicitly. To this end, we relate the magnetization and the density via $m = 1 - 2\rho$ and identify the spontaneous magnetization $m_0 = 1 - 2\rho_0$ as well as, from the symmetry of the Ising model, $\rho_L = 1 - \rho_0$. In addition, we find the magnetic susceptibility $\chi = \hat{\kappa}$ and $\tau_W^{\text{Is}} = 4\tau_W$, due to the shift in the energy scale when exploiting the equivalence of the Ising model and the lattice gas model [10]. Thus, we obtain

$$f(m, T^{\text{Is}}) = \frac{1}{2} \left(1 - \frac{m}{m_0(T^{\text{Is}})} \right) \left(\frac{2m_0(T^{\text{Is}})^2}{\chi(T^{\text{Is}})\tau_W^{\text{Is}}(T^{\text{Is}})} \right)^{\frac{d}{d+1}}, \quad (7)$$

with $T^{\text{Is}} = 4T$ when rewriting the Hamiltonian according to the definition in Sec. III and Ref. [10].

In two dimensions, the involved quantities are known analytically or up to arbitrary precision: m_0 is described by the Onsager-Yang equation [17], χ is obtained from sufficiently long series expansions [18–20] and $\tau_W^{\text{Is}} = 2\sqrt{W}$ can be obtained from the volume of the Wulff plot W [21]. For a collection of equations we refer to Ref. [9]. We numerically evaluated Eq. (7) in Eq. (3), fixing the density and volume and solving with a bisection algorithm for the corresponding transition temperature. We will compare this result to the numerical finite-size results later in Fig. 6 (top) and refer to it as the full solution of Eq. (3).

In three dimensions, we may make use of low-temperature series expansions of the spontaneous magnetization [22]. This allows us to estimate the infinite-system transition temperature T_0 by solving $\rho - \rho_0(T) = 0$. We will compare these results to the finite-size scaling fits of our numerical data and refer to it as the solution from low-temperature series expansion in Fig. 6 (center).

The analytic results may be used to recapture the scaling of the droplet size at condensation, where the fraction λ_c will be in the largest droplet. For the volume of the droplet at condensation it follows $\delta V_D = (\rho_L - \rho_0)^{-1} \lambda_c \delta N_c$ [4], where the total particle excess at condensation δN_c encodes the shape of the droplet [see Eq. (2)]. In general, the volume of an ideal droplet may be expressed by $\delta V_D = S_d R^d$, where S_d is a geometric shape factor that allows to describe both spherical and cubic droplets, where the latter may occur in lattice systems below the roughening transition [10]. Equating both droplet volumes, inserting δN_c from Eq. (2), and solving for the radius yields

$$R = (S_d^{-1} \delta V_D)^{\frac{1}{d}} \propto V^{\frac{1}{d+1}}, \quad (8)$$

consistent with results in the literature [6,7]. For fixed density, this is equivalent to $R \propto N^{1/(d+1)}$. Moreover, the leading finite-size scaling corrections in Eq. (5) may be expressed in powers of R^{-1} , i.e., $T_c - T_0 \propto R^{-1}$.

B. Rounding of the droplet condensation-evaporation transition

In analogy, one may argue that the rounding of the transition at fixed density should scale with the system size in the same way as the rounding of the transition density (or magnetization) at fixed temperature. The latter was derived by Binder [6] using a phenomenological theory. He predicted a finite-size rounding proportional to $V^{-d/(d+1)}$. Starting from a two-state approximation the discussion may be reduced to a homogeneous and an inhomogeneous phase. Then, the rounding of the transition may be related to a characteristic width $\beta\Delta F$ of order unity, where ΔF is the free-energy difference between both phases.

Expanding the free-energy difference $\beta\Delta F$ around the finite-size transition temperature T_c , recalling that $(\partial/\partial\beta)\beta F = E$, yields

$$\beta\Delta F = (\beta\Delta F)|_{T_c} - \left(\frac{1}{k_B T^2} \Delta E \right) \Big|_{T_c} (T - T_c) + \dots \quad (9)$$

The free-energy difference vanishes at T_c in the limit of large system sizes, considering that both phases contribute with equal probability. In the gas phase, the particles may be considered noninteracting. Thus, the energy difference is dominated by the droplet energy, which depends on the droplet volume $\propto R^d$. At T_c , Eq. (8) relates the droplet radius R to the system volume and the energy difference may be approximated to leading order as $\Delta E \sim V^{d/(d+1)}$. The finite-size corrections from the transition temperature appear merely as corrections to the energy difference, such that Eq. (9) simplifies to $\beta\Delta F \sim (V^{d/(d+1)}/k_B T_0^2)\Delta T$ in the limit of large system sizes. The condition $|\beta\Delta F| \sim 1$ yields to leading order the rounding width $\Delta T \propto V^{-d/(d+1)}$ and in terms of the particle number

$$\Delta T \propto N^{-\frac{d}{d+1}}. \quad (10)$$

Notice that the radius of the droplet R as relevant length scale was used in the argumentation such that for large system sizes the rounding may be identified as $\Delta T = T - T_c \propto R^{-d}$.

III. MODELS AND METHODS

In order to investigate the universal aspects of the condensation-evaporation transition, we employ two different particle gas models, for a sketch see Fig. 2. Bridging the gap to analytic solutions [4], we consider a lattice gas model equivalent to the Ising model at fixed magnetization [8,15]. We add to our investigation a Lennard-Jones gas model, which—in

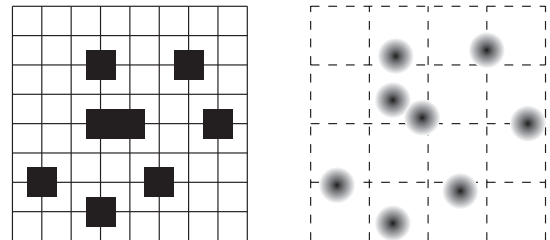


FIG. 2. Sketch of the particle gas models under investigation: The discrete lattice gas model (left) in two and three dimensions and the continuous Lennard-Jones gas model with domain decomposition (right) in three dimensions.

contrast to the lattice gas—is not symmetric with respect to particle-hole exchange (see also Refs. [11,13]). The boundary conditions are periodic, which is common for a finite-size scaling analysis. That way, nonintended interactions with the boundaries are avoided. For both models, we consider a finite interaction range smaller than the linear extension of the system, which safely allows the use of periodic boundary conditions.

A. Lattice gas

In the discrete lattice gas (DLG) model, particles are described by occupied sites on a two-dimensional (2D) square or three-dimensional (3D) cubic lattice of size $V = L^d$. The interaction is purely short range, with attraction between nearest neighbors and hard-core repulsion by the condition that each site can be occupied by only one particle. Introducing a state variable for each site, $n_i \in \{0, 1\}$, the Hamiltonian may be written as

$$\mathcal{H}_{\text{DLG}} = - \sum_{(i,j)} n_i n_j, \quad (11)$$

equivalent to the Ising model ($s_i \in \{\pm 1\}$) at fixed magnetization if $n_i = \frac{1}{2}(s_i + 1)$. Here, the density $\rho = N/V$ can only be adjusted approximately by occupying an integer number of sites $N = \rho L^d$.

B. Lennard-Jones gas

The Lennard-Jones gas (LJG) model is a continuous particle gas model, where in principle all particles interact with each other via the potential

$$V_{\text{LJ}}(r_{ij}) = 4\epsilon \left[\left(\frac{\sigma}{r_{ij}} \right)^{12} - \left(\frac{\sigma}{r_{ij}} \right)^6 \right], \quad (12)$$

with $\epsilon = 1$ and $\sigma = 2^{-1/6}$ such that the potential minimum is at $r_{\text{min}} = 1$. Being consistent with literature and reducing the computational demand, we introduce a cut-off radius $r_c = 2.5\sigma$ above which the potential is zero. The remaining potential is then shifted by $V_{\text{LJ}}(r_c)$ in order to be continuous:

$$V_{\text{LJ}}^*(r) = \begin{cases} V_{\text{LJ}}(r) - V_{\text{LJ}}(r_c) & r < r_c \\ 0 & \text{else} \end{cases}. \quad (13)$$

That way, we may use a domain decomposition, only calculating interactions with particles in neighboring domains. This reduces the computational demand especially in the gas phase. The Hamiltonian is given by

$$\mathcal{H}_{\text{LJG}} = \frac{1}{2} \sum_{i \neq j} V_{\text{LJ}}^*(r_{ij}). \quad (14)$$

Here, we consider only the three-dimensional case of particles in a cubic box of size $V = L^3$ with periodic boundary conditions and $L = (N/\rho)^{1/3}$.

For the present study, we considered the Lennard-Jones gas with the same density as for the lattice gas. The Lennard-Jones gas may be reasonably applied to nonpolar gases, for example argon (Ar). For this case, molecular dynamics simulations were matched with experiments already in the 1960s [23]. Corresponding parameters are $\sigma \approx 3.4 \text{ \AA}$ and $\epsilon/k_B \approx 120 \text{ K}$,

which serve well for an order-of-magnitude comparison. This would lead to a real temperature $T^{\text{real}} = T\epsilon/k_B$. In order to compare to the literature boiling point, the density would have to be adjusted accordingly, e.g., for argon, $T_{\text{boiling}} \approx 87.3 \text{ K}$ [24] with a gas density $\rho_{\text{boiling}} \approx 5.772 \text{ g/l}$ at atmospheric pressure. The unit length a in our system is related to the parametrized length scale as $a = 2^{1/6}\sigma$. Assuming a molar weight of $39.95 \times 1.6605 \times 10^{-27} \text{ kg}$ for argon, this yields the conversion for the density $\rho^{\text{real}} \approx \rho \times 1.226 \times 10^3 \text{ g/l}$. In dimensionless units, the experimental boiling (evaporation) temperature and gas density yield $T_0 \approx 0.728$ and $\rho \approx 0.005$, respectively.

C. Parallel multicanonical simulations

The droplet condensation-evaporation transition shows a phase coexistence between a supersaturated gas phase and a mixed phase consisting of a droplet and a remaining gas phase. The resulting free-energy barrier [5,25] decreases the probability to pass from one phase to the other in the canonical ensemble, which leads to effects such as hysteresis and other effects characteristic for first-order-like phase transitions. In order to overcome these barriers and to sample the transition point with high accuracy, we apply multicanonical simulations [26,27]. This is a natural choice for the fixed-density scheme, while for fixed-temperature a similar approach is not straightforward. The Boltzmann weight $\exp(-\beta E)$, where $\beta = (k_B T)^{-1}$ with $k_B = 1$, is replaced by an *a priori* unknown weight function, which is iteratively modified in order to yield a flat histogram [27]. This allows the sampling of suppressed states between the coexisting phases and produces accurate estimates of the observables when reweighting around the transition temperature. As a result, we obtain a full temperature range from a single simulation applying standard time-series and histogram reweighting techniques.

However, this requires us to sample a broad energy range with sufficiently many tunnel events across the transition point from high energy to low energy and vice versa. We make use of a parallel implementation of the multicanonical method [28], which allows a reduction of computational time. In the cases of lattice gas condensation, it was tested and shown to speed up the simulation by the number of cores used [10]. We considered lattice sizes up to 1000^2 for the 2D and 100^3 for the 3D lattice gas as well as Lennard-Jones particle systems with up to 512 particles with a fixed density $\rho = 10^{-2}$. The Monte Carlo updates in the lattice systems include local particle shifts to a nearest-neighbor site combined with particle displacements to a random new site. For the Lennard-Jones gas, we restrict ourselves to local random particle displacements.

D. Metropolis simulations

In addition, we applied standard Metropolis simulations in order to sample the droplet phase at coexistence. We can use the finite-size scaling corrections from the fit to the transition temperatures obtained with the parallel multicanonical simulations. Then, we make use of the first-order nature of the transition causing a suppression of the intermediate states between the vapor and the mixed phase. Preparing a system in the droplet phase, the Metropolis simulation thermalizes

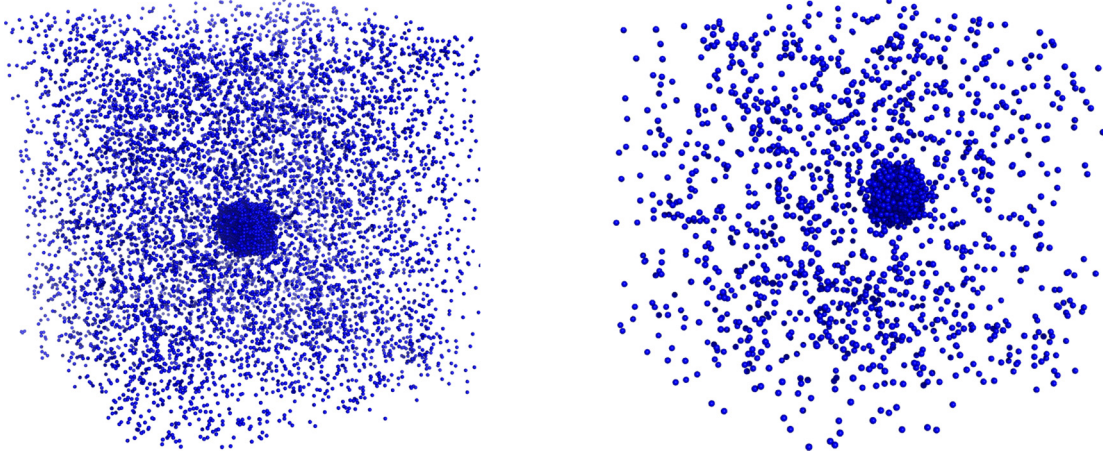


FIG. 3. (Color online) Example of equilibrium droplets at coexistence from Metropolis simulations for the 3D lattice gas with $N = 10\,000$ (left) and the 3D Lennard-Jones gas with $N = 2\,000$ (right).

and only samples the droplet phase for a finite time. With increasing system size, this finite time gets larger and we may safely sample the size of the critical droplet with a lot less statistics than would be required for the multicanonical simulation. However, we need the multicanonical data of suitable system sizes in order to obtain valid estimates of the transition temperature. We do not use the Metropolis data to draw conclusions about the transition temperature or the finite-size rounding but instead directly measure the critical droplet size. This allows us to reach an additional order of magnitude in N . An example for the 3D cases is shown in Fig. 3.

E. Observables

The focus of this study lies on two observables and their thermal derivatives, namely the energy E and the fraction of particles in the largest cluster $\eta = N_D/N$. The latter is determined by identifying the largest cluster as the maximal number of connected particles N_D . In case of the lattice gas, the connected particles are simply nearest neighbors. For the Lennard-Jones gas particles are defined as connected if $r_{ij} < 2\sigma$. Thus, η is a measure of the mass of the largest

droplet and allows one to study the homogeneous nucleation transition efficiently. An example for the 3D Lennard-Jones gas is given in Fig. 4 (left). The consideration of these types of geometric clusters is a safe choice for dilute systems. Note that for rather dense lattice systems also the stochastic Swendsen-Wang cluster definition has been considered [29].

Anticipating a first-order phase transition, we expect in the thermodynamic limit a discontinuity in the energy as well as in η . Hence, the thermal derivatives of the observables $\frac{d}{dT} O = k_B \beta^2 (\langle E O \rangle - \langle E \rangle \langle O \rangle)$ will show a pronounced peak at the transition temperature T_c for finite systems, see Fig. 5. The determination of the peak may be done very precisely due to the full temperature range from multicanonical simulations. The error is estimated by using jackknife error analysis [30], where we make use of the independent parallel production runs combining all but one time series for each jackknife bin. In the case of the energy, the thermal derivative is related to the specific heat $C_V = k_B \beta^2 (\langle E^2 \rangle - \langle E \rangle^2)/N$.

Moreover, we will use the mass fraction η in order to directly verify the predictions about the scaling of the critical droplet size that was assumed and used in the theory. We want to focus on the droplet phase and estimate the average fraction of particles in the largest cluster at the

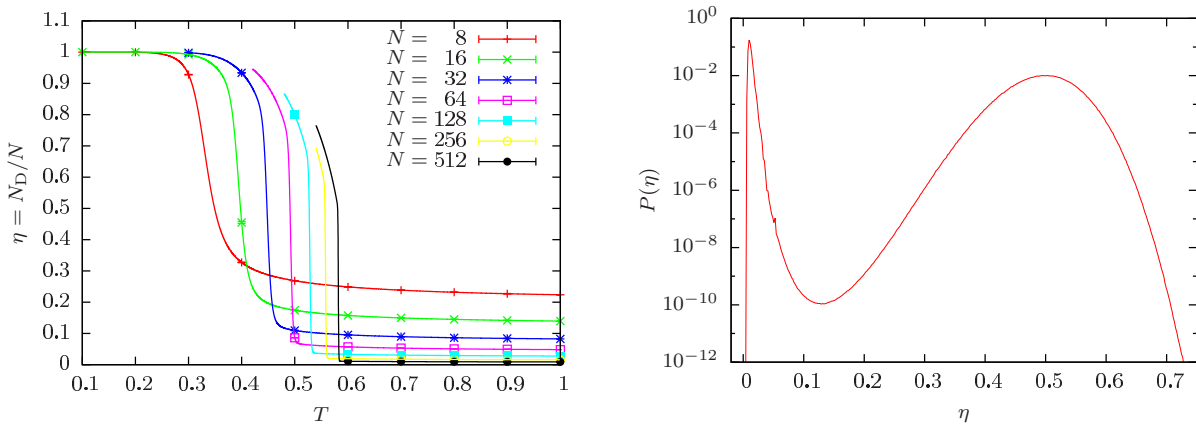


FIG. 4. (Color online) Canonical estimates of the fraction η of particles in the largest droplet for a 3D Lennard-Jones gas at fixed density $\rho = 10^{-2}$ (left). Corresponding probability distribution of η at T_c for $N = 512$ (right).

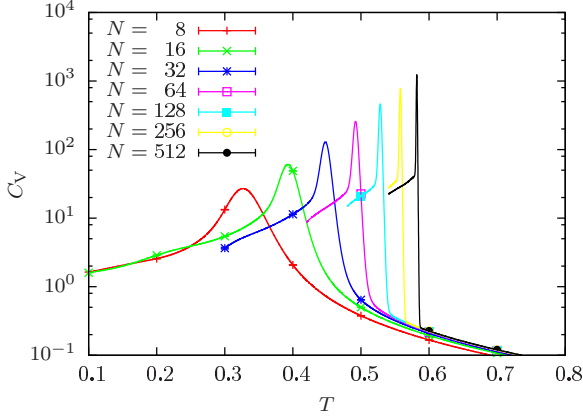


FIG. 5. (Color online) Canonical estimates of the specific heat from parallel multicanonical simulations of the 3D Lennard-Jones gas at fixed density $\rho = 10^{-2}$.

transition temperature $\langle \tilde{\eta} \rangle_{T_c}$. To this end, we reweight our multicanonical data to droplet size distributions $P(\eta)$ by time-series reweighting, adding each reweighting factor to the histogram bin corresponding to the observable. An example is shown in Fig. 4 (right). Assuming that both phases are at equal weight, we identify η_{\min} such that $\tilde{Z} = \int_{\eta_{\min}} d\eta P(\eta) = 0.5$. Then

$$\langle \tilde{\eta} \rangle_{T_c} = \frac{1}{\tilde{Z}} \int_{\eta_{\min}} d\eta \eta P(\eta)|_{T_c} \quad (15)$$

is a robust estimator for sufficiently large systems. In fact, we directly deal with the number of particles in a droplet such that the integrals become discrete sums. Errors are again estimated using the jackknife error analysis. Systematic errors may arise from imperfect estimates of the coexistence temperature, the definition of the droplet boundary and, especially for small systems, if the distribution does not show a sufficiently pronounced dip between the two phases.

IV. RESULTS

The results are presented for a fixed particle density $\rho = N/V = 10^{-2}$, up to one exemplary case when comparing the Lennard-Jones transition temperature to the argon boiling point. This choice of a dilute system ensures that the observed transition is really that associated with the formation of a droplet and not of a cylinder or slab [12]. We have to emphasize in the beginning that the lattice model obviously shows discretization effects for small systems because this explicit density may not be realized for any system size and in general remains approximate. We will see, however, that this does not influence our main conclusions.

We consider only a single density, because we want to test the leading-order finite-size corrections and scaling exponents. The density will, however, influence the finite-size scaling limit. In order to illustrate this, consider the low-temperature series expansion of the 3D Ising model. Here, the spontaneous magnetization is given to first order as $m_0 = 1 - 2e^{-12\beta^{1/3}} + \dots$. For $T \rightarrow 0$ or $\rho_0 \rightarrow 0$, this yields for the density $\rho_0 = \frac{1}{2}(m_0 - 1) = e^{-3\beta}(1 + \dots)$ and to first order for the inverse temperature $\beta \simeq -\frac{1}{3} \ln \rho_0$. This result

may be similarly deduced from microcanonical arguments in continuous systems (see Ref. [2]).

A. Finite-size scaling of the droplet condensation-evaporation transition temperature

The transition temperature, where the transition-related observables show a discontinuity, may be estimated by the peak locations of their thermal derivatives, for an example see Fig. 5. In the limit of large systems, this transition temperature is predicted to scale as

$$T_c = T_0 + aN^{-\frac{1}{d+1}} + \dots, \quad (16)$$

see Sec. II A. Figure 6 shows numerical results for the three considered situations, the lattice gas in two and three dimensions and the Lennard-Jones gas in three dimensions. The estimated transition temperatures are obtained from the maxima of the specific heat (red pluses) as well as the thermal derivative of the fraction of particles in the largest cluster $\frac{d\eta}{dT}$ (green crosses). Both estimates are remarkably similar as expected for first-order phase transitions, and hence we only show local fits to the estimated transition temperature derived from the specific heat.

In all three cases, we observe for large system sizes a proper finite-size scaling behavior according to the predicted scaling, shown by a good quality of the least-squares fits (a reduced χ^2 per degree of freedom of about 1). In accordance with the literature, we verify that this requires rather large system sizes for the leading order fit (dashed dark blue fit). The intermediate-sized systems may be included in an empirical fit with the next higher orders (dotted light blue fit), i.e., $T_c = T_0 + aN^{-1/(d+1)} + bN^{-2/(d+1)}$. In addition, we want to mention that for intermediate system sizes an effective different scaling behavior may be observed. While not completely apparent, it may be justified by sufficiently good χ^2 , that the transition temperature can be locally describes by a $N^{-1/d}$ behavior (dash-dotted orange fit). For details of the individual fits see Table I and the following discussion. The scaling of the intermediate regime is consistent with studies of flexible homopolymer aggregation [2], where a large fraction of the system is involved in the formation of the droplet or aggregate. If almost all constituents are involved in the transition, then the linear extension of the homogeneous, isotropic condensate is just $N^{1/d}$, which justifies the assumed scaling behavior. This leads to two possible conclusions: Either the local scaling function is a polymer property or it is a generic property for a small number of polymers, where the latter seems to be in agreement with the presented results. In order to explore this observation further, we will investigate the size of the critical droplet and the rounding of the transition (which in fact provides suitable fitting ranges for the transition temperature) in the following subsections.

In the case of the 2D lattice gas, we may compare directly to the analytic solution of the infinite system and to the full solution of Eq. (3) for finite systems derived in Sec. II A. The full solution shows large deviations for small systems as expected. With increasing system size, however, it starts to describe the finite-size scaling approximately. This already gives a hint to the choice of a proper fitting range with a leading-order scaling behavior. A least-square fit of the

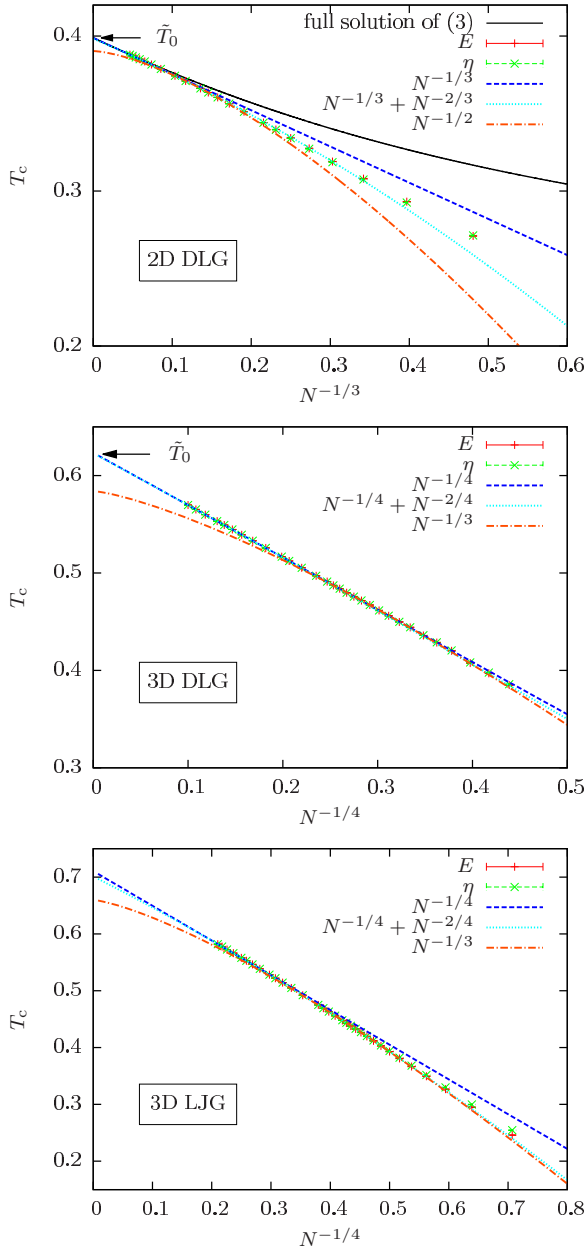


FIG. 6. (Color online) Finite-size scaling of the condensation-evaporation transition temperature for the 2D lattice, 3D lattice, and 3D Lennard-Jones gas from top to bottom. The lattice gas is compared to theoretical predictions (see text and also Sec. II A).

leading order for the largest system sizes $N \geq 2500$ yields an adequate $\chi^2 \approx 0.4$ and an infinite-size transition temperature $T_0 = 0.39884(3)$. This is consistent with the analytic result inverting Onsager's solution for the magnetization [17], with $T = T^{\text{ls}}/4$,

$$m_0(\tilde{T}_0) = 0.98 = [1 - \sinh^{-4}(1/2\tilde{T}_0)]^{1/8}. \quad (17)$$

The resulting $\tilde{T}_0 = 0.39882$ is shown in Fig. 6 (top) by the arrow. Including the next order and fitting $N \geq 400$ yields a $\chi^2 \approx 1.8$ with $T_0 = 0.3982(1)$, which slightly deviates from the exact solution. This may be taken as a hint that our next-order term is only an effective correction and additional corrections of the same order may be apparent. Interesting to compare is also the amplitude of the leading-order correction $aN^{-1/3}$. The linear and higher order fits yield $a = -0.234(1)$ and $a = -0.214(2)$ respectively. This may be compared to the power-series expansion of the full solution [see Eq. (5) and Eq. (7)]. Making use of the analytic solution for m_0 , the series expansion for χ up to three-hundredth order and the integral solution of τ_w (for a list of equations see Ref. [9]), we may numerically differentiate Eq. (7) and calculate in lattice gas units $a = \Delta_c^{2/3} \rho^{1/3} / 4f'(m, T_0^{\text{ls}}) \approx -0.239$ in decent agreement with the leading-order fit. The previously mentioned intermediate scaling regime is not very prominent for the 2D lattice gas where a least-square fit to $N^{-1/2}$ in the (already small) range $N = [324, 900]$ still yields a $\chi^2 \approx 8$. Moreover, the infinite-size extrapolation is obviously wrong. It is worth noting, that the intermediate scaling regime in polymer aggregation [2] was observed in three dimensions, which suggests that the prominence of this regime may depend on the dimension.

For the 3D lattice gas, we may compare the finite-size scaling results of the infinite-size transition temperature to low-temperature expansions, see Sec. II A. A fit of the leading-order scaling behavior to sufficiently large systems in the range $N \geq 2160$ yields $T_0 = 0.62341(4)$ with $\chi^2 \approx 0.6$, which is in the vicinity of the (not exact) low-temperature expansion $\tilde{T}_0 \approx 0.622$ [22], again shown by the arrow. Increasing the fit range still yields reasonably good fits with higher χ^2 of the same quality as the fit including the next order $N^{-2/4}$, see also Table I. Notice that in the case of the 3D lattice gas also the small system sizes seem to coincide with the leading-order fit. However, considering only an intermediate regime allows to fit the $N^{-1/3}$ behavior with qualitatively good local agreement.

TABLE I. Results of different fit functions to the condensation-evaporation transition temperature with the statistical errors of the fits. If no upper range is provided, it refers to $N_{\text{max}} = 10000$ for the lattice gas cases (2D and 3D) and $N_{\text{max}} = 512$ for the Lennard-Jones gas. The reference infinite-size value \tilde{T}_0 is obtained for the lattice systems from the Onsager solution (2D) [17] and from low-temperature series expansions (3D) [22].

| Model | $T_0 + aN^{-1/(d+1)}$ | | | $T_0 + aN^{-1/(d+1)} + bN^{-2/(d+1)}$ | | | $T_0 + aN^{-1/d}$ | | | Ref |
|--------|-----------------------|------------|----------|---------------------------------------|-----------|----------|-------------------|-----------|----------|-----------------|
| | Range | T_0 | χ^2 | Range | T_0 | χ^2 | Range | T_0 | χ^2 | |
| 2D DLG | [2500:] | 0.39884(3) | 0.4 | [400:] | 0.3982(1) | 1.8 | [324:900] | 0.3903(2) | 8.0 | 0.39882... |
| 3D DLG | [2160:] | 0.62341(4) | 0.6 | [1663:] | 0.6229(4) | 1.9 | [68:243] | 0.5840(3) | 1.6 | ≈ 0.622 |
| 3D LJG | [160:] | 0.7106(4) | 0.8 | [10:] | 0.7011(4) | 1.1 | [12: 48] | 0.6597(4) | 1.0 | |

If the larger system sizes were not present, this could be interpreted as the leading order scaling behavior. Comparing the fit to this effective ansatz with the low-temperature series expansion shows, however, strong deviations.

In the case of the 3D Lennard-Jones gas one may best see the arising peculiarities. The leading-order fit for $N \geq 160$ to $N^{-1/4}$ yields $T_0 = 0.7106(4)$ with $\chi^2 \approx 0.8$ but shows a clear deviation for small system sizes. Including the next order for $N \geq 10$ yields $T_0 = 0.7011(4)$ with $\chi^2 \approx 1.1$, in rough agreement with the leading-order result, and recaptures the deviation of the small system sizes. This is consistent with results for the same Lennard-Jones model [31,32]. However, considering an intermediate regime $N = [12:48]$ with the ansatz $N^{-1/3}$ yields a qualitatively good fit with $T_0 = 0.6597(4)$ and $\chi^2 \approx 1$, which deviates strongly from the $N^{-1/4}$ fit. Again, if the largest system sizes were not present this could be interpreted as the finite-size scaling corrections, especially if no reference temperature is available. Locally it seems that this is an intermediate scaling regime which is, however, already covered by the theoretically predicted scaling behavior including empirical higher-order corrections. This shows the necessity to control that the available data is really in the expected leading-order scaling regime.

Comparing to the boiling temperature of argon, we have to exemplary consider a density $\rho = 5 \times 10^{-3}$. Then, the leading-order fit yields $T_0 = 0.6525(3)$ (not shown here), which differs from the experimental result $\tilde{T}_0 \approx 0.728$ (see Sec. III B) by $\sim 10\%$. While the order of magnitude is comparable, the difference is expected for the truncated Lennard-Jones potential [31].

The largest systems considered for the Lennard-Jones gas included 512 particles in a box of length $L \approx 37.1 \approx 41.7\sigma$. This is a lot smaller than the system sizes considered in Ref. [13] ($L \leq 100\sigma$) at fixed temperature $T \approx 0.68$ (for their parametrization) with typical particle numbers $N \approx 15\,800$. Still, in this fixed- T approach they did not see the predicted scaling behavior of the transition density shift but needed to extrapolate an effective exponent (smaller than -0.89) in order to recover the theoretical prediction $L^{-0.75}$. Similarly, a direct fit of the leading-order power-law exponent to the present data yields $N^{-0.28(1)} \propto L^{-0.84(2)}$ already for smaller system sizes $N \geq 160$. This implies that an orthogonal phase boundary crossing may lead in certain situations to reduced finite-size corrections and serves as a useful, complementary approach.

B. Finite-size rounding of the droplet condensation-evaporation transition

In the limit of large systems, the rounding of the transition is predicted to scale as $\Delta T \propto N^{-d/(d+1)}$ for fixed density, see Sec. II B. Figure 7 shows the rescaled specific heat from Fig. 5 for the 3D Lennard-Jones gas. At a first-order transition, the maximum of the specific heat should scale inverse proportional to the rounding of the transition [33]. The rounding of the transition is here estimated as the half width of the specific-heat peak, defined as the width where $C_V \geq \frac{1}{2} C_V^{\max}$. Errors are obtained by jackknife error analysis.

Figure 8 shows the finite-size scaling of the rounding for all three considered systems. In all cases, we could clearly

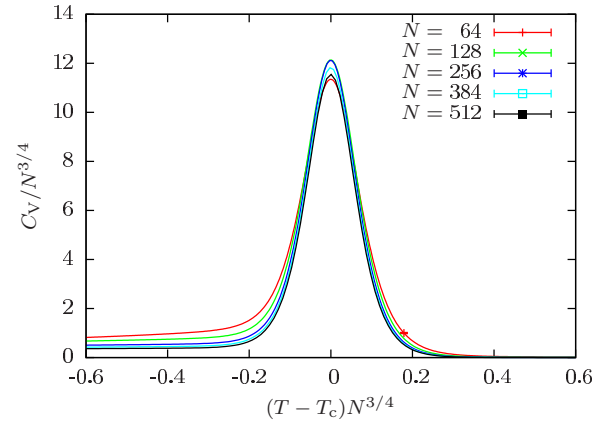


FIG. 7. (Color online) Example of the transition rounding for the specific heat of the 3D Lennard-Jones gas. The x and y axes are rescaled according to the leading-order scaling behavior.

identify two different scaling regimes: For intermediate system sizes one may observe $\Delta T \propto N^{-1}$ (dashed line) and for large system sizes $\Delta T \propto N^{-d/(d+1)}$ (solid line). The latter is the expected scaling of the rounding as predicted by theory [6,13] and reformulated in Sec. II B. Thus, having only data available in the intermediate regime would suggest a wrong finite-size scaling behavior consistent with the intermediate regime for the transition temperature. However, the intermediate regime is nicely fitted by considering the predicted scaling behavior for large system sizes and empirically including the next-higher-order corrections (dash-dotted light blue fit), i.e., $\Delta T = a' N^{-d/(d+1)} + b' N^{-2d/(d+1)}$.

In the case of the 2D lattice gas, smallest systems show no systematic behavior which explains the large deviations in Fig. 6. For the intermediate regime one can see a direct particle or volume dependence (ρ fixed). The onset of the large-system regime is consistent with the scaling range in the transition temperature that approximately coincides with the full solution (Fig. 6). A fit including higher-order corrections yields a $\chi^2 \approx 0.7$ including already system sizes $N \geq 324$ and thus including the intermediate regime.

For the 3D lattice gas and the Lennard-Jones gas, the intermediate regime is apparent for quite small systems and also shows the N proportionality up to the crossover to the large-system regime. Again, the crossover is consistent with a good choice of a leading-order fitting range for the finite-size scaling of the transition temperature. The fit to the rounding of the transition, including higher-order corrections, allows to include system sizes $N \geq 175$ with $\chi^2 \approx 2.3$ for the lattice gas and $N \geq 16$ with $\chi^2 \approx 0.9$ for the Lennard-Jones gas case. Again, this includes (parts of) the intermediate regime by considering empirical higher-order corrections.

Previous studies of the lattice gas in two and three dimensions at fixed ρ showed significant deviations from the predicted exponents for the transition rounding [14], using average densities of states from Wang-Landau simulations. For the 3D case they found an effective scaling of the rounding with $L^{-2.45(2)} \propto N^{-0.82(1)}$. The present results on the other hand clearly confirm the large-system scaling behavior. Direct fits of the power-law behavior to the largest system sizes of the

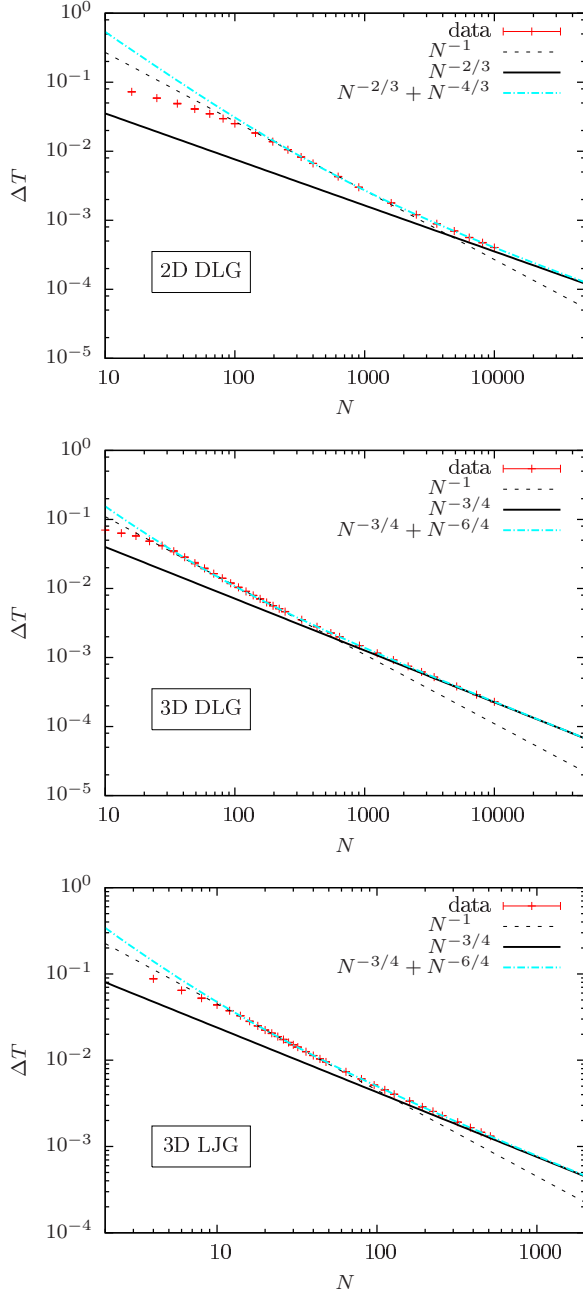


FIG. 8. (Color online) Finite-size rounding of the droplet condensation-evaporation transition for the 2D lattice, 3D lattice, and 3D Lennard-Jones gas from top to bottom. The results are presented for $\rho = 0.01$ but are consistent for different densities.

3D lattice gas model yield effective exponents $N^{-0.78(1)}$ and $N^{-0.76(1)}$ for $N \geq 1663$ and $N \geq 5120$, respectively, close to the predicted scaling $N^{-0.75}$.

The finite-size rounding shows to be a good observable to identify the previously noticed intermediate regime. The width of the transition is associated to the fluctuations of the system [33], which should depend on the inverse volume of the relevant system size. The relevant system size remains the droplet, which scales for large systems as $R^d \propto N^{d/(d+1)}$. On the other hand, for small systems the droplet includes a large fraction of the system, see the following discussion. Thus

the local scaling of the intermediate regime is not surprising. Knowing the scaling behavior for large systems, however, allows to anticipate this gradual crossover with empirical higher-order corrections.

C. Scaling regimes of the critical droplet size

We identified the leading-order finite-size scaling corrections as powers of the critical droplet radius. This requires that the mass of the critical droplet scales in the limit of large systems as $N^{d/(d+1)}$. We want to test this relation by considering the fraction of particles in the largest cluster η —or in other words the mass of the droplet divided by the total number of particles—that should scale as $N^{-1/(d+1)}$.

Figure 9 shows that this assumption seems to be valid for all three considered models. In each case, we show the expectation value $\langle \tilde{\eta} \rangle_{T_c}$ in the droplet phase at the transition temperature. The horizontal dashed line at $\eta = 1$ corresponds to all particles being in the droplet. For one, the results from our multicanonical simulation (red pluses) are measured as described in Sec. III E with jackknife errors. In addition, there are statistical averages from canonical Metropolis simulations (green crosses) prepared in the droplet phase at $T_c(N) = T_0 + aN^{-1/(d+1)}$ as extrapolated in Sec. IV A. To be precise, we considered the following pairs (T_0, a) : $(0.623, -0.537)$ for the 3D lattice gas as well as $(0.710, -0.611)$ for the 3D Lennard-Jones gas. In this case, the errors are statistical errors including the integrated autocorrelation times. The straight line is the expected scaling behavior shifted as a guide to the eye in order to be compared with the numerical data.

The 2D lattice gas shows the expected scaling behavior quite early, already for roughly 100 particles. In the case of the 3D lattice gas the situation already changes and the expected scaling behavior only starts for quite large system sizes of the order of 2000 particles. This is consistent with the 3D Lennard-Jones gas, where, however, the available system sizes are much smaller. Still the expected scaling may be anticipated. Including the Metropolis data, it shows that the leading-order extrapolation of the available transition temperatures is not precise enough and seems to overestimate the transition temperature for larger systems, consistent with the observations in Sec. IV A.

All cases show that for small system sizes, the majority of particles is included in the single macroscopic droplet. A corresponding constant behavior $\langle \tilde{\eta} \rangle_{T_c} \sim 1$ (the horizontal dashed line) would explain an intermediate scaling regime where the relevant length scale depends on the system volume. From Fig. 9, this may be at most guessed locally. However, regarding the measurement of the average critical droplet we have to mention that the small systems including only a few particles also show narrow distributions. These are discretized by nature and only defined in the range $[1, N]$. Thus, the observable may not provide the required measurement sensitivity. Still, having a large fraction of particles in the droplet, especially compared to the vanishing fraction in the limit of large systems, suffices for the argument that locally an effective intermediate scaling becomes visible. Moreover, it becomes clear that there are corrections to the size of the critical droplet for small and intermediate systems. This should

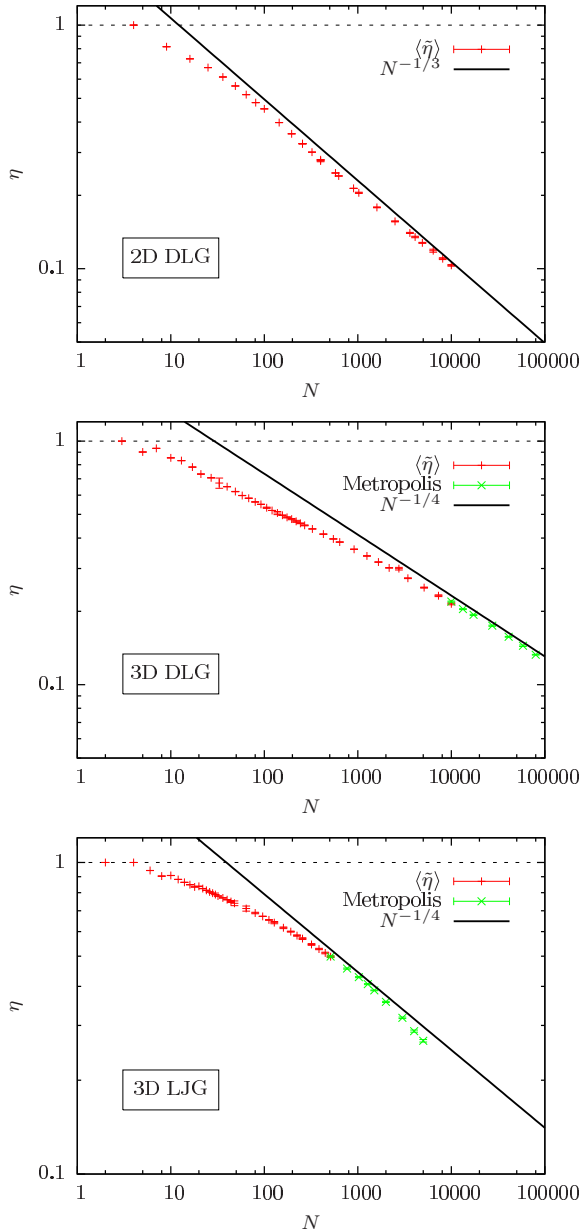


FIG. 9. (Color online) Scaling of the particle fraction in the largest droplet η for the 2D lattice, 3D lattice, and 3D Lennard-Jones gas from top to bottom. For large systems, η should scale as $N^{-1/(d+1)}$. For small system sizes, the majority of particles is in the droplet $\eta = \mathcal{O}(1)$ (horizontal dashed line). The Metropolis data are obtained in the droplet phase at the finite-size transition temperature as extrapolated from the linear fit in Fig. 6.

also have an effect on the scaling of the transition temperature and rounding.

V. CONCLUSIONS

We presented results on the canonical finite-size scaling of the droplet condensation-evaporation transition. To this end, we performed a comparative study in which we considered two- and three-dimensional lattice gas as well as three-

dimensional off-lattice Lennard-Jones gas models in order to draw general conclusions. In all cases, we could verify the theoretical predictions about the finite-size corrections to the transition temperature $\propto N^{-1/(d+1)}$ and the finite-size rounding $\propto N^{-d/(d+1)}$ in the limit of large systems [4,6]. In addition, we identified an intermediate regime with an effective different scaling behavior in all three cases, most apparent in the finite-size rounding. This regime is consistent with results from flexible polymers [2], where the aggregate included most of the polymers. Our measurement of the average droplet size in equilibrium with vapor at coexistence showed that indeed for small system sizes a large fraction of the system is included in the single macroscopic droplet. The scaling of the droplet size, however, is nicely described by the theoretical predictions [6,7] in the limit of large systems.

Without knowledge of the larger system sizes, the intermediate regime could give way to a wrong finite-size scaling behavior with qualitatively good fit results for both the transition temperature and rounding. However, we were able to show that there is a gradual crossover to the large-system scaling regime which can be approximately described by including empirical higher-order corrections to the theoretical scaling predictions, namely polynomial orders of the critical droplet size. If only the leading-order corrections are considered, the rounding is a good source getting a lower fit limit for a qualitatively good fit. This was compared to analytic and low-temperature results for the lattice cases. It is thus also suitable in order to identify the finite-size scaling regime for phase transitions with mixed phases, such as the condensation-evaporation transition but also more complex systems such as polymer aggregation. Considering only the local, intermediate regime and applying standard finite-size scaling approaches (with possibly wrong corrections) would then lead to wrong estimates of the infinite-system limit. A similar note of caution has been recently demonstrated in the finite-size scaling of self-avoiding walks on percolation clusters [34].

An intuitive approach to the leading-order finite-size scaling corrections is the competition of volume (L^d) and surface (L^{d-1}) contributions. For a first-order phase transition, this gives rise to a finite-size correction of the order L^{-1} , where L is the relevant length scale of the system [2,35–37]. We argue that the linear extension of the droplet R at coexistence plays this dominant role. The condensation-evaporation transition clearly connects a homogeneous and a mixed phase in the canonical ensemble. However, within the canonical approach, we may consider a (virtual) subsystem with the volume of the transition droplet. By translational invariance, this subsystem may be always constructed around the largest droplet. Above the transition temperature, this subsystem includes a homogeneous gas phase while at and below the transition it is filled by the largest droplet and hence shows a homogeneous liquid phase. Thus, this may be interpreted as a grand-canonical transition between homogeneous phases in the virtual system spanned by the volume of the critical droplet. By construction, this virtual volume would have open boundary conditions yielding a finite-size shift of order R^{-1} and a finite-size rounding of order R^{-d} . This picture is consistent with rigorous results for nonperiodic first-order phase transitions [37]. However, this argument relies on the

finite-size scaling of $R \propto N^{1/(d+1)}$, which was shown to be already nontrivial.

The present study shows that considering an orthogonal crossing of the phase boundary still yields the same finite-size corrections and serves as a complementary tool. On the example of the transition rounding, the fixed-density approach was shown to be closer to the expected large-system scaling behavior already for smaller system sizes. In general, both directions have their advantages and drawbacks both numerically and systematically. This may be exploited for one's benefit by choosing the suitable direction for the problem at hand, as was also recently demonstrated for the Blume-Capel model [38].

ACKNOWLEDGMENTS

We thank A. Malakis, M. Mueller, and P. Schierz for useful discussions. The project was funded by the European Union and the Free State of Saxony. Computing time provided by the John von Neumann Institute for Computing under Grant No. HLZ21 on the supercomputer JUROPA at Jülich Supercomputing Centre is gratefully acknowledged. Part of this work has been financially supported by the Deutsche Forschungsgemeinschaft (DFG) through the Leipzig Graduate School of Excellence GSC185 "BuildMoNa" and by the Deutsch-Französische Hochschule (DFH-UFA) through the German-French Graduate School under Grant No. CDEA-02-07.

-
- [1] F. Müller-Plathe, *ChemPhysChem* **3**, 754 (2002).
- [2] J. Zierenberg, M. Mueller, P. Schierz, M. Marenz, and W. Janke, *J. Chem. Phys.* **141**, 114908 (2014).
- [3] M. Mueller, W. Janke, and D. A. Johnston, *Phys. Rev. Lett.* **112**, 200601 (2014).
- [4] M. Biskup, L. Chayes, and R. Kotecký, *Europhys. Lett.* **60**, 21 (2002); *Commun. Math. Phys.* **242**, 137 (2003).
- [5] T. Neuhaus and J. S. Hager, *J. Stat. Phys.* **113**, 47 (2003).
- [6] K. Binder, *Physica A* **319**, 99 (2003).
- [7] K. Binder and M. H. Kalos, *J. Stat. Phys.* **22**, 363 (1980).
- [8] A. Nußbaumer, E. Bittner, T. Neuhaus, and W. Janke, *Europhys. Lett.* **75**, 716 (2006).
- [9] A. Nußbaumer, E. Bittner, and W. Janke, *Phys. Rev. E* **77**, 041109 (2008).
- [10] J. Zierenberg, M. Wiedenmann, and W. Janke, *J. Phys.: Conf. Ser.* **510**, 012017 (2014).
- [11] L. G. MacDowell, P. Virnau, M. Müller, and K. Binder, *J. Chem. Phys.* **120**, 5293 (2004).
- [12] L. G. MacDowell, V. K. Shen, and J. R. Errington, *J. Chem. Phys.* **125**, 034705 (2006).
- [13] M. Schrader, P. Virnau, and K. Binder, *Phys. Rev. E* **79**, 061104 (2009).
- [14] S. S. Martinos, A. Malakis, and I. Hadjiagapiou, *Physica A* **384**, 368 (2007).
- [15] M. Pleimling and A. Hüller, *J. Stat. Phys.* **104**, 971 (2001).
- [16] M. Kastner and M. Pleimling, *Phys. Rev. Lett.* **102**, 240604 (2009).
- [17] L. Onsager, *Nuovo Cimento (Suppl.)* **6**, 261 (1949); C. N. Yang, *Phys. Rev.* **85**, 808 (1952).
- [18] W. P. Orrick, B. G. Nickel, A. J. Guttmann, and J. H. H. Perk, *Phys. Rev. Lett.* **86**, 4120 (2001); *J. Stat. Phys.* **102**, 795 (2001).
- [19] B. Nickel, *J. Phys. A: Math. Gen.* **32**, 3889 (1999); **33**, 1693 (2000).
- [20] S. Boukraa, A. J. Guttmann, S. Hassani, I. Jensen, J.-M. Maillard, B. Nickel, and N. Zenine, *J. Phys. A: Math. Theor.* **41**, 455202 (2008); Y. Chan, A. J. Guttmann, B. G. Nickel, and J. H. H. Perk, *J. Stat. Phys.* **145**, 549 (2011).
- [21] K. Leung and R. K. P. Zia, *J. Phys. A: Math. Gen.* **23**, 4593 (1990).
- [22] M. F. Sykes, J. W. Essam, and D. S. Gaunt, *J. Math. Phys.* **6**, 283 (1965); G. Bhanot, M. Creutz, and J. Lacki, *Phys. Rev. Lett.* **69**, 1841 (1992).
- [23] A. Rahman, *Phys. Rev.* **136**, A405 (1964).
- [24] Ch. Tegeler, R. Span, and W. Wagner, *J. Phys. Chem. Ref. Data* **28**, 779 (1999).
- [25] A. Nußbaumer, E. Bittner, and W. Janke, *Prog. Theor. Phys. Suppl.* **184**, 400 (2010).
- [26] B. A. Berg and T. Neuhaus, *Phys. Lett. B* **267**, 249 (1991); *Phys. Rev. Lett.* **68**, 9 (1992).
- [27] W. Janke, *Int. J. Mod. Phys. C* **03**, 1137 (1992); *Physica A* **254**, 164 (1998).
- [28] J. Zierenberg, M. Marenz, and W. Janke, *Comput. Phys. Comm.* **184**, 1155 (2013).
- [29] F. Schmitz, P. Virnau, and K. Binder, *Phys. Rev. E* **87**, 053302 (2013).
- [30] B. Efron, *The Jackknife, the Bootstrap and other Resampling Plans* (Society for Industrial and Applied Mathematics, Philadelphia, 1982).
- [31] A. Trokhymchuk and J. Alejandro, *J. Chem. Phys.* **111**, 8510 (1999).
- [32] G. A. Chapela, G. Saville, S. M. Thompson, and J. S. Rowlinson, *J. Chem. Soc., Faraday Trans. 2* **73**, 1133 (1977).
- [33] Y. Imry, *Phys. Rev. B* **21**, 2042 (1980).
- [34] N. Fricke and W. Janke, *Phys. Rev. Lett.* **113**, 255701 (2014).
- [35] V. Privman and J. Rudnick, *J. Stat. Phys.* **60**, 551 (1990).
- [36] C. Borgs and R. Kotecký, *J. Stat. Phys.* **79**, 43 (1995).
- [37] C. Borgs, R. Kotecký, and I. Medved, *J. Stat. Phys.* **109**, 67 (2002).
- [38] J. Zierenberg, N. G. Fytas, and W. Janke, *Phys. Rev. E* **91**, 032126 (2015).